Critical Phenomena in Fluid Invasion of Porous Media

Nicos Martys,[a] Marek Cieplak,[b] and Mark O. Robbins
Department of Physics and Astronomy, Johns Hopkins University, Baltimore, Maryland 21218
(Received 27 April 1990)

We present a phase diagram for fluid invasion of porous media as a function of pressure P and the contact angle θ of the invading fluid. Increasing P leads to percolation above a critical θ_c, and depinning below θ_c. Depinning is characterized by a diverging coherence length and the power-law distribution of events typical of self-organized critical phenomena. At the transition from percolation to depinning another correlation length diverges and an order parameter, an effective macroscopic surface tension, becomes nonzero. The fluid interface changes from self-similar to self-affine. Results are compared to experiments.

PACS numbers: 47.55.Mh, 64.60.−i, 68.10.Cr, 68.10.Gw

Studies of fluid invasion, displacement of one fluid by an immiscible fluid in a porous medium, have revealed a wealth of interesting pattern-formation processes.[1-6] In many cases, invasion at low flow rates is well described by the invasion percolation model:[2] Segments of the interface in each pore advance independently along the path of least resistance, leading to a fractal invasion pattern. However, recent work[5-8] indicates that this behavior is not universal. In particular, as the invading fluid becomes more wetting, cooperative invasion mechanisms may lead to totally different growth processes and morphology.

In this paper, we present the first theoretical study of cooperative invasion. We show that the invaded pattern is compact rather than fractal. The interface is self-affine, and our calculated roughness exponent agrees well with recent experiments.[3,4] As suggested by other experiments,[8] we find that the onset of continuous flow is characteristic of a depinning transition like those in charge-density-wave (CDW) conductors, flux lattices, and other systems.[9] The range over which growth is coherent diverges at the transition, and the distribution of invaded areas has the "$1/f$" form characteristic of self-organized critical phenomena.[10] Finally, we show evidence for an effective macroscopic surface tension Γ, which acts at scales larger than the pore size. The existence of a macroscopic tension has been an important open issue in theories of viscous fingering in porous media.[1,6,11,12] Γ is only nonzero when growth is cooperative, and its magnitude behaves like an order parameter describing the transition from fractal to compact growth.

Simple model two-dimensional (2D) porous media were constructed by placing disks of random radii on a square or triangular lattice with lattice constant a. The system size was $1000a$ or more in each direction. Results below are for a triangular lattice with r/a uniformly distributed between 0.05 and 0.49. They are representative of other systems studied.

At low velocities, invasion is dominated by capillary effects: the surface tension γ of the fluid interface, and the wetting properties of the fluids. The latter are described[13] by the static contact angle θ of the invading fluid which varies from 180° to 0° as the fluid changes from nonwetting to wetting. We model quasistatic invasion as a stepwise process where each unstable section of the interface moves to the next stable or nearly stable configuration in turn. The algorithm is described in detail in Ref. 7. A fixed pressure drop P is applied across the interface, which consists of a sequence of circular arcs connecting pairs of disks (Fig. 1). Stable arcs must have radius γ/P and intersect the disks at θ.

Three types of instability are identified: "burst"—no arc with radius γ/P intersects both disks at θ, "touch"—an arc connecting two disks intersects a third, and "overlap"—arcs between successive pairs of disks intersect. As θ decreases, the dominant instability changes from bursts to overlaps. Bursts and touches are local mechanisms which can be included in percolation mod-

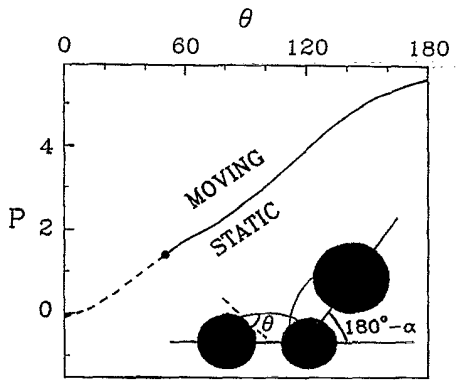

FIG. 1. Typical (θ,P) phase diagram for quasistatic invasion. Solid (dashed) lines indicate P_c for percolation (depinning). The solid circle indicates θ_c. Results are symmetric for $P \leftrightarrow -P$ and $\theta \leftrightarrow 180° - \theta$ which corresponds to reversing both flow direction and fluids. Inset: Arcs between two successive pairs of beads on an interface. The invading fluid is below the interface and θ and α are measured as indicated.

els.[1,2] In contrast, overlap depends on the configuration of adjacent arcs. As can be seen from Fig. 1, overlap becomes more likely as the bond angle α between successive disks decreases. Thus, overlaps smooth the interface and lead to cooperative motion.

For each θ we identify a critical pressure P_c at which interfaces first span an infinite system. A typical (θ,P) phase diagram is shown in Fig. 1. In the nonwetting limit (large θ) each throat between pores is invaded independently, leading to fractal patterns as predicted by the invasion percolation model.[1,2] The cooperative overlap mechanism becomes increasingly important as the invading fluid becomes more wetting. The width w of coherently invaded regions diverges[7] as θ decreases to a critical angle θ_c. We now show that growth for $\theta < \theta_c$ is characteristic of a depinning transition.

Figure 2 illustrates the dramatic difference in growth morphology as $P \to P_c$ for (a) $\theta = 25°$ and (b) $\theta = 90°$, which are below and above $\theta_c \simeq 49°$, respectively. The lower interface in each case was stable at a pressure about 1% below P_c. P was increased slightly until a single arc became unstable. The black region shows the area A invaded as the fluid advanced to the next stable interface. Above θ_c, the fluid follows the tortuous path of least resistance typical of percolation. There are many trapped regions where the invading fluid has surrounded the displaced fluid. Below θ_c, a large segment of the interface moves forward coherently, and there is little trapping.

A measure of the degree of coherence is $\langle \lambda^2 \rangle$, the mean squared Cartesian width of the segments of the interface which advance due to single instabilities (Fig. 2) in a given pressure range. Below θ_c, $\langle \lambda^2 \rangle$ diverges at P_c (Fig. 3): *The entire interface advances coherently.* The mean area invaded, $\langle A \rangle$, also diverges. As expected for compact growth, we find $\langle \lambda^2 \rangle \propto \langle A \rangle \propto (P_c - P)^{-\phi}$ with $\phi = 2.30 \pm 0.05$. In contrast, $\langle \lambda^2 \rangle^{1/2} \approx 5a$ for all P at $\theta = 90°$—each segment of the interface advances almost independently. $\langle A \rangle$ diverges, but with an exponent $\phi = 1.75 \pm 0.10$, which can be related to percolation exponents. Details of the finite-size scaling determinations of these and other exponents, as well as scaling relations between them, will be presented in a longer paper.

Recent work has recognized that many systems organize themselves into a critical state at the onset of flow.[9,10] Examples include CDWs,[9] sandpiles,[10] and the earthquake faults.[14] The characteristic signatures of self-organized critical phenomena are a diverging coherence length and a power-law distribution of events. Figure 3 illustrates the divergence of $\langle \lambda^2 \rangle$ as $P \to P_c$ below θ_c. At P_c we find power-law distributions ρ of A and λ^2. Over nearly six decades in area, both distributions functions are fitted by $\rho(y) \propto y^{-\tau}$, with $\tau = 1.125 \pm 0.025$. Above θ_c, A has a power-law distribution with $\tau = 1.35 \pm 0.10$.

The onset of flow for $\theta < \theta_c$ seems most analogous to the depinning transitions in charge-density-wave conductors and related systems.[8] The ingredients which yield depinning transitions in these systems are a random local force η and an elastic coupling. Segments of the system (interface) are pinned with different strengths by η. In the absence of an external force F (here P), many configurations of the system are stable. As F increases, regions which are weakly pinned become unstable and advance. This increases the elastic force on neighboring regions, which may in turn depin. As F increases to a threshold value F_c, the number of stable configurations of the interface decreases to zero, and the cascades pro-

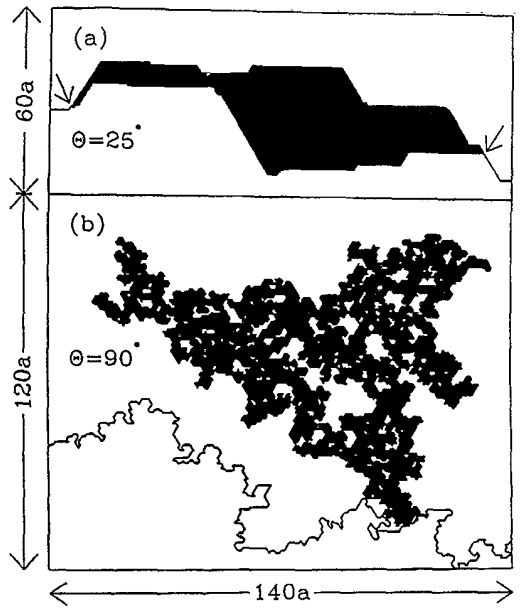

FIG. 2. Area A invaded (black) when a single arc became unstable at the indicated θ and $(P_c - P)/P_c \sim 0.01$. λ is the Cartesian width of the advancing interface segment [distance between arrows in (a)].

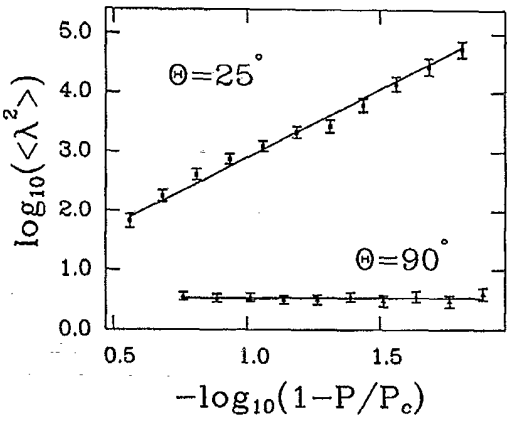

FIG. 3. Variation of $\langle \lambda^2 \rangle$ with P for $\theta = 90°$ and 25°. Solid lines are power-law fits with slopes 0 and 2.3 for $\theta = 90°$ and 25°, respectively.

duced by each instability diverge.[9] For $F > F_c$ the entire system advances.

In fluid invasion the porous medium provides the random field. There is some experimental evidence for an elastic coupling,[3,5,6,8] but there has been no microscopic explanation of its origin. The decrease with α in the pressure for instability through overlap (Fig. 1) provides such an explanation. When one section of the interface advances, the values of α on either side decrease. These adjacent regions are thus more unstable, and a single instability may cause a cascade. Viewed another way, regions with net positive curvature κ (invading fluid surrounded) have fewer small-α bonds and thus become unstable at higher P. Regions of negative κ (displaced fluid surrounded) have more small-α bonds and become unstable at lower P. If the change in pressure scales linearly with κ, the coefficient Γ has units of surface tension. Like a normal surface tension, Γ relates the curvature of a region to the pressure at which it *advances*. Unlike a microscopic surface tension, Γ is not related to the onset of *backward flow* which occurs through mechanisms corresponding to nonwetting invasion at a much different P.

We have verified the existence of Γ numerically. Many random initial interfaces were chosen. P was increased gradually until P_f, the pressure where the fluid invaded the entire system. The radius of gyration R_G of the last stable interface was used to determine the average curvature: $\kappa = +1/R_G$ for growth outward from a central ring, and $\kappa = -1/R_G$ for growth into a surrounded circle. In Fig. 4 we plot P_f vs κ for a large number of starting rings at $\theta = 25°$. As expected, local variations in the medium produce different depinning thresholds. However, the linear trend of P_f with κ is clearly seen. A least-mean-squares fit yields $\Gamma = 1.05\gamma$ and all points lie within lines given by 0.5γ and 2γ.

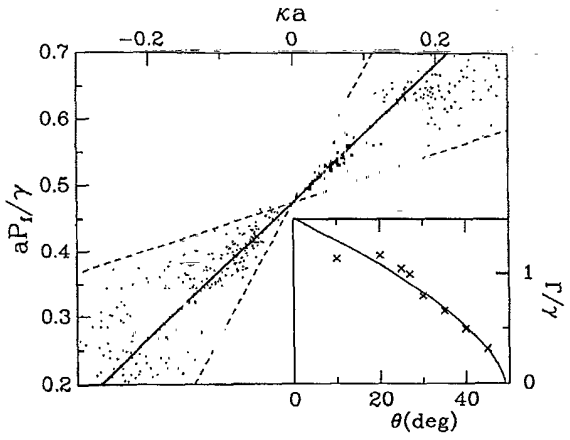

FIG. 4. Plot of P_f vs κ for many initial interfaces at $\theta = 25°$. The mean slope $\Gamma = 1.05\gamma$ (solid line). Fluctuations are bounded by dashed lines. Inset: Numerical values of Γ as a function of θ (crosses) and a power-law fit (solid line).

The value of Γ varies with θ like an order parameter describing the transition from percolation to depinning at θ_c (Fig. 4, inset). Above θ_c, we find $\Gamma = 0$, and below, $\Gamma \sim (\theta_c - \theta)^\beta$ with $\beta = 0.6 \pm 0.2$. Since Γ is zero above θ_c, there is no smoothing force. Thus the large-scale structure at P_c is self-similar. As shown in Ref. 7, the fractal dimensions of the bulk and external perimeter are consistent with normal percolation:[1] $\frac{91}{48}$ and $\frac{4}{3}$, respectively. Experimental studies of nonwetting invasion also reveal self-similar fractal structure.[1,5]

Below θ_c, the nonzero value of Γ exerts a powerful large-scale coherence and at P_c the fluid interface is self-affine.[1] To determine[3] the Hurst roughness exponent H we calculated the rms deviation $h(x)$ from a straight line as a function of the projected line length x. Figure 5 presents a plot of $\log_{10} h(x)$ vs $\log_{10} x$ obtained by averaging results from stable interfaces in twelve different systems at $\theta = 25°$. The results lie on a straight line over one and a half decades. The slope, $H = 0.81 \pm 0.05$, gives the roughness exponent [$\bar{h}(x) \propto x^H$]. The major uncertainty comes from small overhangs on some interfaces. Including such regions lowers the apparent value of H at small x.

One implication of self-affine structure is that the interface has a well-defined average orientation.[1] To quantify this we calculated the surface normal correlation function S at several values of θ. The limiting value at large distances, $S(\infty)$, is zero for $\theta > \theta_c$. Below θ_c, $S(\infty)$ behaves like an order parameter and is roughly proportional to Γ.

Two recent experiments on wetting invasion have measured the roughness exponent of interfaces moving at low velocities U. Rubio *et al.*[3] found $H = 0.73 \pm 0.03$. Horváth, Family and Vicsek[4] initially reported a much higher value, ~ 0.9, but their more recent work gives $H \approx 0.81$. These exponents agree remarkably well with our simulation results, while most growth models give $H = 0.5$ in 2D. An exception is the Kardar, Parisi, and Zhang model with power-law-correlated noise.[15] It has been unclear how such noise might arise. We suggest

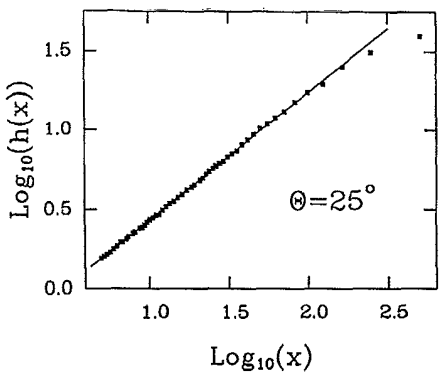

FIG. 5. Mean of $\log_{10} h(x)$ vs $\log_{10} x$ for $\theta = 25°$ (squares) and a power-law fit (line) with slope 0.81.

that the power-law distribution of invaded areas at P_c naturally introduces an analogous effect. The observed H would then be associated with the critical point and only hold up to $\sim\lambda$. This is consistent with our simulations. Viscous effects should also be important at sufficiently large scales.[1,6] Flattening in the experimental plots of $h(x)$ vs x at large x and high U may reflect this influence.[3]

If the invading fluid is less viscous, the dominance of viscous effects at large scales results in viscous fingering.[6,11] One theory for the fingerwidth ζ assumes that an effective macroscopic surface tension stabilizes the interface.[6,12] Linear stability analysis then predicts a maximally unstable wavelength proportional to $\mathrm{Ca}^{-0.5}$, where $\mathrm{Ca}=\mu U/\Gamma$ is the capillary number and μ the viscosity of the more viscous fluid. In experiments on wetting invasion, ζ is proportional to this wavelength, but for nonwetting invasion ζ is always of the order of the pore size. Our results provide a ready explanation for this dichotomy: $\Gamma\sim\gamma$ for wetting invasion and vanishes for nonwetting invasion. Note that one also observes[6,11] spatial variation in ζ. This is consistent with the spread induced in Fig. 4 by local fluctuations.

A full theory for the magnitude of ζ must include other important effects. For example,[1,12] nonlinear effects coarsen fingers, and noise leads to tip splitting that limits ζ. The velocity dependence of the capillary pressure P_{cap} may also play an important role.[11]

From the above discussion, it is clear that the transition from percolation to depinning at θ_c shows many similarities to equilibrium second-order phase transitions. Disorder in the bead pack acts like thermal noise. Overlaps provide a coupling between neighboring arcs on the interface, causing them to act cooperatively. As θ decreases, the relative strength of the coupling increases and a correlation length w diverges[7] at θ_c. Below θ_c, the long-range orientational order implied by $S(\infty)>0$ is analogous to long-range spin correlations in a ferromagnet or the orientational order in an uncrumpled membrane.[16] It remains to be seen whether a formal mapping to such equilibrium transitions (like that between the zero-state Potts model and percolation) exists.

We thank J. R. Banavar, A. Dougherty, F. Family, J. P. Gollub, J. P. Stokes, D. A. Weitz, and D. Wilkinson for useful discussions. Support from National Science Foundation Grant No. DMR-8553271 and Petroleum Research Foundation Grant No. 22013-AC6,7 is gratefully acknowledged. M.O.R. also acknowledges support from the Sloan Foundation.

[a]Current address: National Institute of Standards and Technology, 226/B348, Gaithersburg, MD 20899.

[b]Permanent address: Institute of Physics, Polish Academy of Sciences, 02-668 Warsaw, Poland.

[1]See, e.g., J. Feder, *Fractals* (Plenum, New York, 1988).

[2]R. Lenormand and S. Bories, C. R. Acad. Sci. Ser. B **291**, 279 (1980); R. Chandler, J. Koplik, K. Lerman, and J. F. Willemsen, J. Fluid Mech. **119**, 249 (1982).

[3]M. A. Rubio, C. Edwards, A. Dougherty, and J. P. Gollub, Phys. Rev. Lett. **63**, 1685 (1989); **65**, 1389 (1990).

[4]V. K. Horváth, F. Family, and T. Vicsek, Phys. Rev. Lett. **65**, 1388 (1990); (to be published).

[5]R. Lenormand and C. Zarcone, in *Proceedings of the Fifty-Ninth Annual Technological Conference and Exhibition of the Society of Petroleum Engineers, Houston, Texas, 16–19 September 1984* (Society of Petroleum Engineers, Richardson, TX, 1984).

[6]J. P. Stokes, D. A. Weitz, J. P. Gollub, A. Dougherty, M. O. Robbins, P. M. Chaikin, and H. M. Lindsay, Phys. Rev. Lett. **57**, 1718 (1986).

[7]M. Cieplak and M. O. Robbins, Phys. Rev. Lett. **60**, 2042 (1988); Phys. Rev. B **41**, 11508 (1990).

[8]J. P. Stokes, A. P. Kushnick, and M. O. Robbins, Phys. Rev. Lett. **60**, 1386 (1988).

[9]D. S. Fisher, Phys. Rev. Lett. **50**, 1486 (1983).

[10]P. Bak, C. Tang, and K. Wiesenfeld, Phys. Rev. Lett. **59**, 381 (1987); Phys. Rev. A **38**, 364 (1988).

[11]D. A. Weitz, J. P. Stokes, R. C. Ball, and A. P. Kushnick, Phys. Rev. Lett. **59**, 2967 (1987).

[12]G. Li and L. M. Sander, Phys. Rev. A **36**, 4551 (1987).

[13]A fluid interface intersects a solid at a θ fixed by surface energies; see P. G. de Gennes, Rev. Mod. Phys. **57**, 827 (1985).

[14]J. M. Carlson and J. S. Langer, Phys. Rev. Lett. **62**, 2632 (1989).

[15]M. Kardar, G. Parisi, and Y.-C. Zhang, Phys. Rev. Lett. **56**, 889 (1986); E. Medina, T. Hwa, M. Kardar, and Y.-C. Zhang, Phys. Rev. A **39**, 3053 (1989).

[16]Y. Kantor, M. Kardar and D. R. Nelson, Phys. Rev. A **36**, 3056 (1987).